Ultrafast Faraday Rotation of Slow Light

A. I. Musorin,[1] M. I. Sharipova,[1] T. V. Dolgova,[1] M. Inoue,[2] and A. A. Fedyanin[1,*]
[1]Faculty of Physics, Lomonosov Moscow State University, Moscow 119991, Russia
[2]Toyohashi University of Technology, Toyohashi 441-8580, Japan
(Received 30 January 2016; revised manuscript received 19 June 2016; published 18 August 2016)

The active control of optical signals in the time domain is what science and technology demand in fast all-optical information processing. Nanostructured materials can modify the group velocity and slow the light down, as the artificial light dispersion emerges. We observe the ultrafast temporal behavior of the Faraday rotation within a single femtosecond laser pulse under conditions of slow light in a one-dimensional magnetophotonic crystal. The Faraday effect changes by 20% over the time of 150 fs. This might be applicable to the fast control of light in high-capacity photonic devices.

DOI: 10.1103/PhysRevApplied.6.024012

I. INTRODUCTION

Slow light is a unique phenomenon related to low group velocity [1]. This phenomenon provides science and technology with a new outlook on fast all-optical information processing [2] and striking physical effects in atomic vapors [3,4], semiconductor quantum systems [5,6], optical waveguides [7,8], and even free space [9]. The light travels at a speed as low as 17 m/s [10] or even stops [11], when interacting with the medium more efficiently in the spectral region of the flat effective light dispersion [12,13], e.g., in photonic crystals [14,15]. Introducing slow-light effects in magnetophotonic crystals [16] makes it possible to obtain magnetic-field control in femtosecond polarization pulse shaping [17–20]. The latter is required in the coherent control of quantum states [21–23], plasma dynamics [24], chemical reactions [25], molecular alignment [26], and terahertz generation [27].

The Faraday effect [28] manifests itself as a light polarization rotating while being transmitted through a medium magnetized parallel to the wave vector. It is governed by the spin-orbit interaction. The angle of rotation θ is generally detected for monochromatic cw light and scales linearly with the material thickness d. In the time domain, θ is proportional to the time of light traversal through the magnetic material; the nonreciprocity of the effect gives credibility to using the Faraday-active medium as a magnetic clock [29]. The Faraday rotation of the wave envelope depends on the difference between the inverse group and phase velocities v_{gr} and v_{ph}, respectively [30]:

$$\theta = \Omega_L \left(\frac{1}{v_{\mathrm{gr}}} - \frac{1}{v_{\mathrm{ph}}} \right) d, \tag{1}$$

where Ω_L is the Larmor frequency. Thus, slow light and Faraday rotation are the direct counterparts that represent the effective time of the light-matter interaction.

Magneto-optical effects are being enhanced in photonic crystals with functional magnetic layers resulting from light localization in the magnetic material [31–34]. Slow light, as an additional mechanism for optical energy compression, allows one to enhance the optical response, for example, nonlinear effects [35–39], Beer-Lambert-Bouguer absorption [40], radiation pressure [41], stimulated Raman scattering [42], and the Sagnac effect [43]. Faraday rotation is also expected to fit in this row [44].

In this paper, we report the experimental observation of time-resolved polarization rotation within a single femtosecond laser pulse under conditions of slow light in magnetophotonic crystals (MPCs).

A schematic illustration of the effect is presented in Fig. 1(b). The femtosecond laser pulse propagates through the one-dimensional magnetophotonic crystal shown in Fig. 1(a). The total Faraday rotation is defined as the rotation of the resultant superposition of the transmitted electric fields that experience multiple reflections. The rotation of each component of the superposition is proportional to the transit time or inversely proportional to the group velocity. Thus, the output polarization rotation is different for the leading and trailing edges of the pulse, and, according to Eq. (1), the rotation angle varies within the pulse. Figures 1(c) and 1(d) show the spectral dependences of the group velocity and the Faraday angle calculated for various numbers of layers in the MPC mirrors using the 4×4 transfer-matrix formalism [30,45,46]. The group velocity and the Faraday rotation are inversely correlated within the entire spectral region: The lower the group velocity is, the higher the Faraday rotation becomes at the same wavelength. In particular, inside the microcavity mode—900 nm—the v_{gr} decreases, whereas θ increases. This effect is more pronounced for structures with many layers and with higher Q factors. In contrast to the literature on dynamics of the Faraday rotation caused by the intrinsic processes in the medium [47,48], in our case the

*fedyanin@nanolab.phys.msu.ru

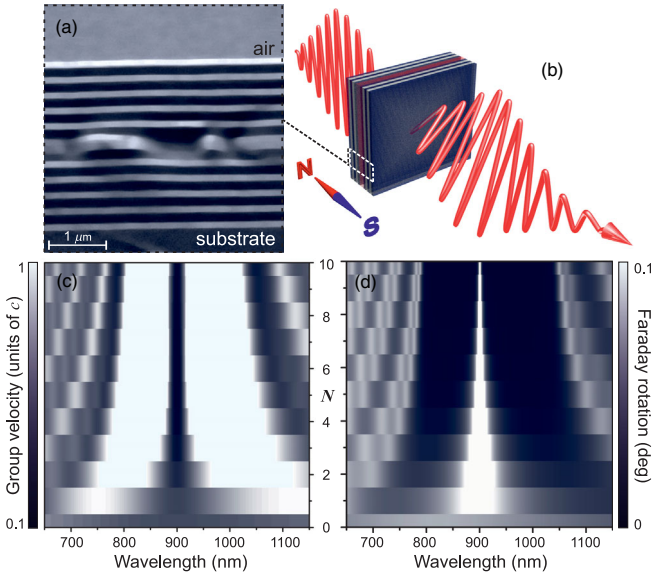

FIG. 1. (a) SEM image of a magnetophotonic crystal. (b) Schematic image of the ultrafast time-dependent polarization rotation in a magnetophotonic crystal. (c) Calculated group velocity and (d) Faraday rotation in the magnetophotonic crystal versus the light wavelength and the number of periods N in the Bragg reflectors.

dynamics is induced by an extrinsic cause—artificial structuring controlling the light dispersion.

II. METHODS AND MATERIALS

A. Polarization-sensitive autocorrelator

The experimental setup combines a polarization-sensitive technique with an autocorrelator of femtosecond pulses [19,49] (see Fig. 2). The polarization-sensitive part allows one to detect polarization rotation [50]. The elements of the scheme before the beam splitter make up the magneto-optical polarimetry. As a light source, we use a visible + IR-range femtosecond Ti:sapphire laser

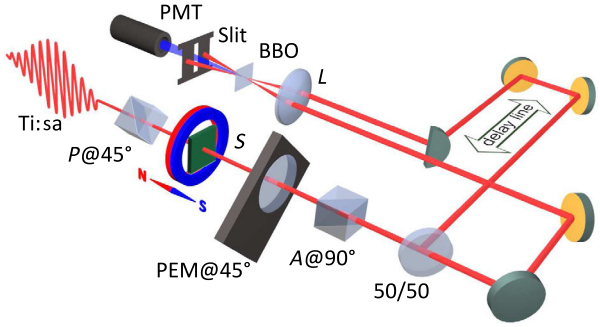

FIG. 2. The experimental setup combines magneto-optical polarimetry with an autocorrelation scheme. Ti:sa, titanium-sapphire laser; P, polarizer; S, sample; PEM, photoelastic modulator; BBO, β-barium borate nonlinear crystal; PMT, photomultiplier tube; L, lens; A, analyzer.

(Chameleon, Coherent Inc.) with an 80-MHz repetition rate, an average intensity of 3000 mW, and an intensity pulse width of 250 fs. A 45°-polarized light pulse passes through the sample at normal incidence (with a beam diameter of approximately 0.5 mm) placed in a constant magnetic field of 1 kOe oriented parallel to the light-propagation direction and then passes through a photoelastic modulator (PEM, Hinds Instruments Inc.), which periodically modulates a polarization rotation that emerges due to the Faraday effect. Then, the pulse passes through a 90°-oriented Glan-Taylor prism, which converts the polarization modulation to the pulse intensity modulation. The latter in the approximation of a small magnitude of Faraday rotation $\theta \ll 1$ can be written as [50]

$$I(t) = I_0(t)[1 + 4J_2\theta(t)\cos(4\pi f t)], \tag{2}$$

where $I_0(t)$ is the temporal profile of the incident light pulse intensity, J_2 is the second-order Bessel function at the argument of 2.405 rad (PEM retardation amplitude used in the experiment), $\theta(t)$ is the time-dependent Faraday rotation, and $f = 47$ kHz is the PEM operating frequency. The correlation part is used for registering the dynamics of the processes. Registering femtosecond pulses requires special techniques, because photodiodes fail to detect such quick processes. One commonly used technique is a second-harmonic-generation correlation scheme. Two variants of this scheme exist: autocorrelation and cross-correlation. The autocorrelation scheme is used in our experiments presented in this paper. The details on polarization-sensitive cross-correlation measurement are given in Ref. [30]. The 50:50 beam splitter splits the laser pulse into two identical beamlets: The first of them passes through a variable delay line, and then both beamlets focus at the same spot into a β-barium borate (BBO) nonlinear crystal. The intensity of the generated noncollinear second harmonic is proportional to the pulse autocorrelation function $u_{ac}(\tau) = \int I(t)I(t-\tau)dt$, where τ is a time delay between the beamlets. If we substitute Eq. (2) into autocorrelation function u_{ac}, we get

$$u_{ac}(\tau) = \underbrace{\int I_0(t)I_0(t-\tau)dt}_{u_{dc}(\tau)} + \cos(4\pi f t)\underbrace{8J_2\int \theta(t)I_0(t)I_0(t-\tau)dt}_{u_{2f}(\tau)}, \tag{3}$$

where u_{dc} and u_{2f} are Fourier amplitudes (at the dc component and at the PEM's double frequency, respectively) of the Fourier transformation of a registered signal. In Eq. (3), we neglect the term proportional to θ^2 because of its infinitesimal value. If the changes in polarization rotation are slower than the pulse duration, i.e., $\dot{\theta}(t) \ll \dot{I}(t)$,

one can consider Faraday-rotation dynamics $\theta(t)$ as being averaged within the pulse—$\theta(t) \simeq \theta(\tau)$ (the dots denote the time derivative). Therefore, the correlation function measured at double PEM frequency is given by the following expression:

$$u_{2f}(\tau) = 8J_2\theta(\tau)\underbrace{\int I_0(t)I_0(t-\tau)dt}_{u_{\rm dc}(\tau)} \equiv 8J_2\theta(\tau)u_{\rm dc}. \quad (4)$$

Consequently, the time dependence of the Faraday rotation can be measured as the ratio of detected locked-in oscillating signal $u_{2f}(\tau)$ to the dc voltage $u_{\rm dc}(\tau)$:

$$\theta(\tau) = \frac{1}{8J_2}\frac{u_{2f}(\tau)}{u_{\rm dc}(\tau)}. \quad (5)$$

If we substitute J_2 for the value $J_2(2.405) = 0.43$, we finally obtain

$$\theta(\tau) = 0.29\frac{u_{2f}(\tau)}{u_{\rm dc}(\tau)}. \quad (6)$$

The resulting expression (6) is given for radians.

B. Sample description

The sample chosen for the experimental observation of a time-resolved Faraday rotation is a MPC, where an anomalous low group velocity is expected at the microcavity mode. The SEM image of the studied MPC is shown in Fig. 1(a). The MPC consists of two dielectric Bragg reflectors and a gyrotropic cavity spacer sputtered on a fused silica substrate [16]. Each reflector is composed of five half-wavelength-thick SiO_2/Ta_2O_5 bilayers. The cavity spacer is a half-wavelength-thick magnetic layer of $Bi_{0.3}Y_{2.7}Fe_5O_{12}$. Figure 3 presents the experimental optical

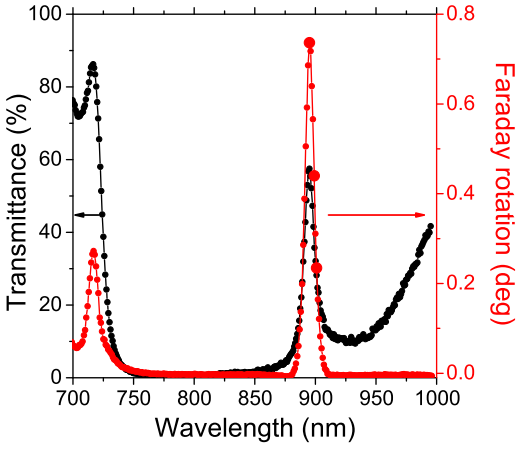

FIG. 3. Spectral dependences of MPC transmittance (black curve) and Faraday rotation (red curve). Large dots mark the wavelengths used for the ultrafast measurements.

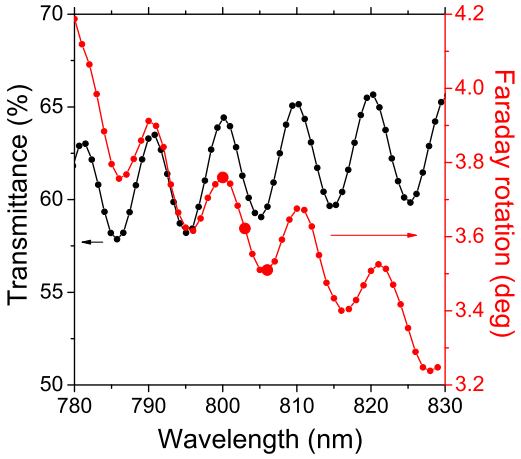

FIG. 4. Transmittance (black curve) and Faraday-rotation (red curve) spectra of a 16-μm-thick magnetic film.

(black curve) and magneto-optical (red curve) spectra of the magnetophotonic crystal. A photonic band gap is observed from approximately 750 to 1000 nm. The microcavity mode is located at 895 nm, shifted to the red region of the spectrum from the photonic-band-gap center, with a transmittance of 67%. The Faraday rotation reaches its maximum value of 0.75° at the microcavity mode with a Q factor of 45.

To relate the effect with the group velocity, we also investigate the reference sample—a magnetic film, which is the extreme case of a MPC with a small Q factor without any Bragg reflectors [see Figs. 1(c) and 1(d) for the case of $N = 0$]. The film is fabricated by the liquid-phase epitaxial growth of a 16-μm-thick $(Bi, Lu, Eu, Tm)_3(Fe, Ga, Al)_5O_{12}$ composite on a $Gd_3Ga_5O_{12}$ substrate. Figure 4 shows the measured spectral dependences of the transmittance (black curve) and Faraday rotation (red curve) of the magnetic film. Although the absolute value of the Faraday rotation exceeds that in the MPC, the specific value (normalized to the thickness of the magnetic material) is one order of magnitude smaller compared with the MPC. The spectra oscillate due to the interference inside the film performing as a Fabry-Perot cavity. The bold dots denote the wavelengths in the vicinity of 800 nm, that have been chosen for the time-resolved measurements. In that area, the Faraday rotation is relatively large—3.76° at 800 nm—and its oscillation amplitude reaches the maximum with a Q factor of 2. The other notable factor is that the maximum of the Ti:sapphire laser output intensity occurs in the vicinity of 800 nm.

III. RESULTS AND DISCUSSION

Figure 5(a) presents the simulated femtosecond dynamics of the Faraday effect in the MPC with a tuning of the central wavelength λ_0 of the femtosecond pulse. The MPC parameters are identical to those of the MPC used in the experiment [30,51–54]. The zero time corresponds to the maximum of the autocorrelation intensity. The Faraday

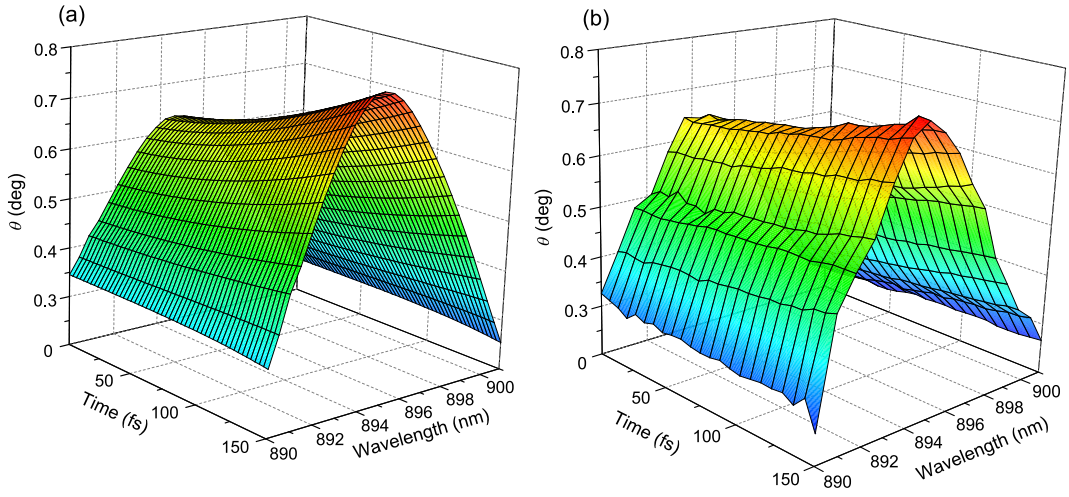

FIG. 5. (a) Calculated and (b) measured Faraday-rotation dynamics of a 250-fs laser pulse with a central wavelength tuning from 890 to 901 nm transmitted through a magnetophotonic crystal.

rotation does not equate zero at zero time, since the light-polarization plane is already rotated after propagating through the magneto-optical material. At the center of the microcavity mode—895 nm—the Faraday rotation increases over the time by approximately $\Delta\theta = 0.15°$ during the first 150 fs. At the mode's edges, 890 and 901 nm, the Faraday rotation remains steady. Consequently, the microcavity peak sharpens with time. The experimental spectral dependence of the time-resolved Faraday effect extracted from the autocorrelation function is shown in Fig. 5(b). The spectral profile of the femtosecond pulse sharpens with time, which is consistent with the numerical data presented in Fig. 5(a).

Figure 6(a) shows the measured (dots) and calculated (curves) time-resolved Faraday rotations for three different pulse central wavelengths: 895 (blue), 899 (green), and 901 nm (red). Figure 6(b) presents the calculated (black curve) and experimental (dots) magneto-optical spectra along with the calculated group velocity (purple curve) in the vicinity of the microcavity mode. The wavelength of 895 nm corresponds to the center of the microcavity mode with the maximum Faraday rotation and with a tenfold decrease in the group velocity. The time-resolved polarization rotation at 895 nm steadily increases by 0.15° over the time interval of 150 fs [see Fig. 6(a), blue]. The instant Faraday rotation reaches the steady-state value at the time of 120 fs and then exceeds it. For a more comprehensive picture, we measure the dynamics of the Faraday rotation for two other pulse central wavelengths, 899 and 901 nm, which are slightly shifted from the center of the microcavity mode (steady-state Faraday rotations equal to 0.43° and 0.23°, respectively). The effect grows in time steadily for the mode slope of 899 nm. However, the increase for 150 fs differs twice: 0.15° at 895 nm versus 0.08° at 899 nm. At the center of the microcavity mode, the group velocity of the light increases, as light is "stored" in the MPC, and some time is required for the light to exit. During this time, the light pulse interacts with the medium and, consequently, leads to the increased Faraday rotation. The steady-state value is achieved relatively late for 895 nm for two main reasons: First, the pulse propagates slower, and its maximum leaves the medium later due to the group-velocity decrease; and second, the rear part of the pulse contributes more to the steady-state value, as it is added constructively to the pulse's lead part.

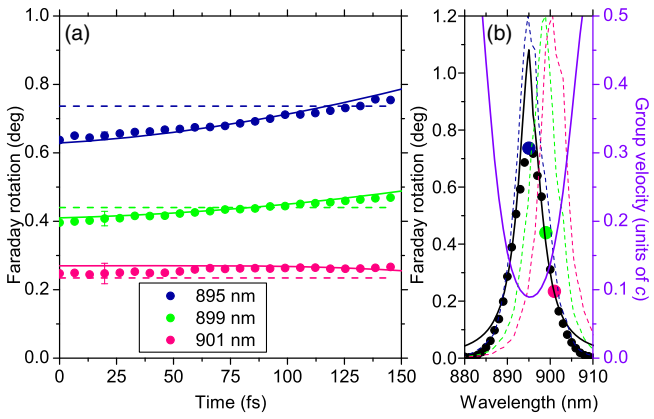

FIG. 6. (a) Faraday-rotation dynamics in a magnetophotonic crystal, experiment (dots) and calculations (curves). Dashed lines indicate steady-state values of the Faraday rotation. (b) Calculated Faraday-rotation (black curve) and group-velocity (purple curve) spectra of the microcavity mode. The dots indicate the measured magneto-optical spectrum. The dashed curves indicate the normalized spectra of the laser pulse at 895 (blue), 899 (green), and 901 nm (red).

The temporal behavior of the Faraday rotation in the thin magnetic film is shown in Fig. 7. The central wavelength of the 250-fs laser pulse tunes from 790 to 810 nm. The time dependence has an oscillating spectral dependence with the same period as the steady-state Faraday-rotation spectrum. The experimental data in Fig. 7(b) coincide with the theoretical simulations, which are shown in Fig. 7(a). Both graphs resemble the surface of a paper fan, where the amplitude of the oscillations increases with time (or distance from the curvature center of the paper fan). Although the oscillation amplitudes increase over

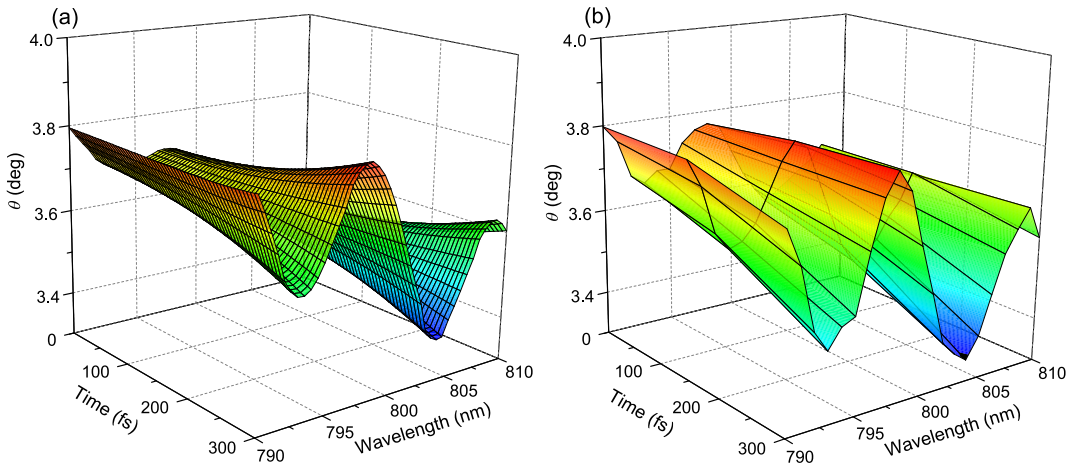

FIG. 7. (a) Calculated and (b) measured Faraday-rotation dynamics of the femtosecond pulse, with the central wavelength varying from 790 to 810 nm, transmitted through a 16-μm-thick magnetic film.

time, the intensity of the rotated light decreases, and only the first 300 fs have an impact on the Faraday-rotation steady-state spectrum.

Figure 8(a) presents the femtosecond dynamics of the Faraday rotation in a magnetic film measured (dots) and calculated (curves) at the maximum (800 nm, blue), minimum (806 nm, red), and midpoint (803 nm, green) of the steady-state Faraday-rotation spectra. In addition, a part of the measured (dots) and calculated (black curve) Faraday-rotation spectra together with the calculated group-velocity (purple curve) spectrum are shown in Fig. 8(b). Owing to the low Q factor, the group velocity varies slightly as related to the wavelength. The instant Faraday rotation is equal to its steady-state value for a pulse with a central wavelength λ_0 of 803 nm. At $\lambda_0 = 800$ nm, the time-resolved Faraday rotation continually increases from 3.7° to 3.8° during 300 fs. The instant Faraday rotation exceeds its steady-state value after approximately 210 fs. At

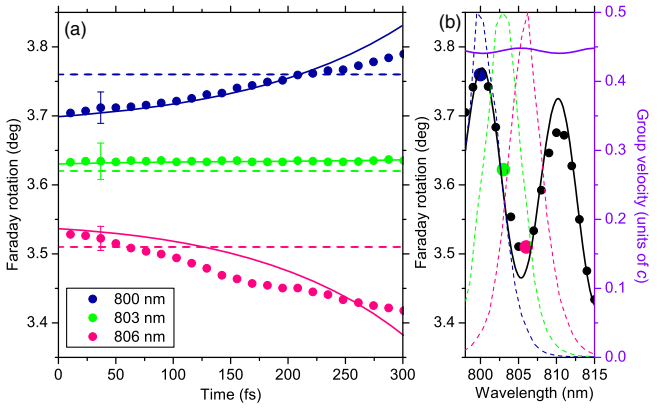

FIG. 8. (a) Time-resolved Faraday rotation in a 16-μm-thick film, experiment (dots) and calculations (curves). Dashed lines mark the steady-state values of the Faraday rotation. (b) Calculated Faraday-rotation (black curve) and group-velocity (purple curve) spectra of the thin magnetic film. The dots are the measured magneto-optical spectrum. The dashed curves indicate the normalized laser spectra at the chosen wavelengths of 800 (blue), 803 (green), and 806 nm (red).

$\lambda_0 = 806$ nm, the time-resolved Faraday rotation continuously decreases by $\Delta\theta = 0.11°$ during the same time period. The instant Faraday rotation becomes smaller than its steady-state value after approximately 80 fs. The conventional view of the Faraday rotation [55] is that it generally increases with time due to the nonreciprocity of the effect. Consequently, the time decay of the Faraday rotation has always been explained by the intrinsic magnetic processes, such as spin relaxation. In our case, the medium's magnetic state remains steady. For the positive derivative of the Faraday rotation, which is observed at 800 nm, the group velocity is lower than average, light spends more time inside the magnetic film, and the output vector of the electric field rotates more and more significantly relative to the initial state. This mode is expected, since the magnetic film is an extreme case of a MPC, with no dielectric mirrors. The time increment of Faraday rotation in the film at the oscillation maximum of 800 nm is comparable to the one in the MPC at the center of the microcavity mode of 895 nm, but the film is thicker by 2 orders of magnitude. The relative change of Faraday rotation normalized to its steady-state value $\Delta\theta/\theta$ differs significantly: 20% for MPC versus 2% for magnetic film. This difference is explained by the difference in the values of the group-velocity decrease. Therefore, the quality factor of the photonic crystal and size of the cavity are ways to control the output time-dependent Faraday effect. In comparison with magnetoplasmonic crystals [56], where the relative change of the femtosecond magneto-optical response is about 8%, the pulse modifies more than that in a MPC and less in magnetic films. An appropriate nanostructure design, for example, with two magnetic layers [57], can lead to the enhanced value of the effect up to 45°. After larger values are obtained, the results would be suitable for practical applications, such as improved magneto-optical spatial light modulators [58] and holographic memory [59]. Another promising implementation is the development of a refractive-index optical sensor. The advantages of a high-sensitivity gyrotropic band-gap sensor [60] will be supplemented by the possibility of an ultrafast

real-time measurement. Finally, the observed effects can be useful for magnetic-field-controlled polarization shaping of ultrafast pulses for coherent control.

IV. SUMMARY AND CONCLUSIONS

In conclusion, in this paper, we detect ultrafast Faraday-rotation dynamics in magnetophotonic crystals caused by femtosecond laser-pulse self-interference in the structured media. The magnitude of the time derivative of the effect depends crucially on the spectral position of the pulse central wavelength with respect to the microcavity mode, due to the artificial light dispersion. The derivative is always positive and is larger when the pulse central wavelength is at the center of the microcavity mode; the farther from the microcavity mode center, the smaller the increase of the Faraday rotation. For the reference film, the time derivative of the Faraday rotation turns from positive to negative via spectral tuning of the incident pulse. For compact magneto-optical devices in data processing, MPCs are more suitable, as the normalized effects are higher than in thin films. The results might be useful for femtosecond polarization pulse shaping with the advantage of magnetic-field control in next-generation photonic devices.

ACKNOWLEDGMENTS

The authors thank Professor A. N. Shaposhnikov for the thin-film sample fabrication and spirited discussions. We also thank N. A. Orlikovskiy for the scanning electron microscopy of the MPC and V. V. Zubyuk for useful comments. This research is supported by the Russian Foundation for Basic Research (Grants No. 16-32-00146, No. 16-32-00902, and No. 16-02-01050).

[1] S. L. McCall and E. L. Hahn, Self-Induced Transparency by Pulsed Coherent Light, Phys. Rev. Lett. **18**, 908 (1967).
[2] A. M. Weiner, *Ultrafast Optics* (Wiley, Hoboken, NJ, 2009).
[3] D. J. Bradley, G. M. Gale, and P. D. Smith, Self-induced transparency and dispersion delays in potassium vapour, Nature (London) **225**, 719 (1970).
[4] B. Gouraud, D. Maxein, A. Nicolas, O. Morin, and J. Laurat, Demonstration of a Memory for Tightly Guided Light in an Optical Nanofiber, Phys. Rev. Lett. **114**, 180503 (2015).
[5] P.-C. Ku, F. Sedgwick, C. J. Chang-Hasnain, P. Palinginis, T. Li, H. Wang, S.-W. Chang, and S.-L. Chuang, Slow light in semiconductor quantum wells, Opt. Lett. **29**, 2291 (2004).
[6] H. Su and S. L. Chuang, Room-temperature slow light with semiconductor quantum-dot devices, Opt. Lett. **31**, 271 (2006).
[7] K. L. Tsakmakidis, T. W. Pickering, J. M. Hamm, A. F. Page, and O. Hess, Completely Stopped and Dispersionless Light in Plasmonic Waveguides, Phys. Rev. Lett. **112**, 167401 (2014).
[8] V. Huet, A. Rasoloniaina, P. Guillemé, P. Rochard, P. Féron, M. Mortier, A. Levenson, K. Bencheikh, A. Yacomotti, and Y. Dumeige, Millisecond Photon Lifetime in a Slow-Light Microcavity, Phys. Rev. Lett. **116**, 133902 (2016).
[9] D. Giovannini, J. Romero, V. Potoček, G. Ferenczi, F. Speirits, S. M. Barnett, D. Faccio, and M. J. Padgett, Spatially structured photons that travel in free space slower than the speed of light, Science **347**, 857 (2015).
[10] L. V. Hau, A. E. Harris, Z. Dutton, and C. H. Behroozi, Light speed reduction to 17 metres per second in an ultracold atomic gas, Nature (London) **397**, 594 (1999).
[11] D. F. Phillips, A. Fleischhauer, A. Mair, R. L. Walsworth, and M. D. Lukin, Storage of Light in Atomic Vapor, Phys. Rev. Lett. **86**, 783 (2001).
[12] J. B. Khurgin and R. S. Tucker, *Slow Light: Science and Applications* (CRC Press, Boca Raton, FL, 2008).
[13] B. Corcoran, C. Monat, C. Grillet, D. J. Moss, B. J. Eggleton, T. P. White, L. O'Faolain, and T. F. Krauss, Green light emission in silicon through slow-light enhanced third-harmonic generation in photonic-crystal waveguides, Nat. Photonics **3**, 206 (2009).
[14] T. Baba, Slow light in photonic crystals, Nat. Photonics **2**, 465 (2008).
[15] K. Kondo and T. Baba, Dynamic Wavelength Conversion in Copropagating Slow-Light Pulses, Phys. Rev. Lett. **112**, 223904 (2014).
[16] M. Inoue, R. Fujikawa, A. Baryshev, A. Khanikaev, P. B. Lim, H. Uchida, O. Aktsipetrov, A. Fedyanin, T. Murzina, and A. Granovsky, Magnetophotonic crystals, J. Phys. D **39**, R151 (2006).
[17] T. Brixner and G. Gerber, Femtosecond polarization pulse shaping, Opt. Lett. **26**, 557 (2001).
[18] A. M. Weiner, Ultrafast optical pulse shaping: A tutorial review, Opt. Commun. **284**, 3669 (2011).
[19] M. R. Shcherbakov, P. P. Vabishchevich, V. V. Komarova, T. V. Dolgova, V. I. Panov, V. V. Moshchalkov, and A. A. Fedyanin, Ultrafast Polarization Shaping with Fano Plasmonic Crystals, Phys. Rev. Lett. **108**, 253903 (2012).
[20] E. Rahimi and K. Şendur, Femtosecond pulse shaping by ultrathin plasmonic metasurfaces, J. Opt. Soc. Am. B **33**, A1 (2016).
[21] D. Press, T. D. Ladd, B. Zhang, and Y. Yamamoto, Complete quantum control of a single quantum dot spin using ultrafast optical pulses, Nature (London) **456**, 218 (2008).
[22] T. Brixner, G. Krampert, T. Pfeifer, R. Selle, G. Gerber, M. Wollenhaupt, O. Graefe, C. Horn, D. Liese, and T. Baumert, Quantum Control by Ultrafast Polarization Shaping, Phys. Rev. Lett. **92**, 208301 (2004).
[23] W. S. Warren, H. Rabitz, and M. Dahleh, Coherent control of quantum dynamics: The dream is alive, Science **259**, 1581 (1993).
[24] Z.-H. He, B. Hou, V. Lebailly, J. A. Nees, K. Krushelnick, and A. G. R. Thomas, Coherent control of plasma dynamics, Nat. Commun. **6**, 7156 (2015).
[25] A. Assion, T. Baumert, M. Bergt, T. Brixner, B. Kiefer, V. Seyfried, M. Strehle, and G. Gerber, Control of chemical reactions by feedback-optimized phase-shaped femtosecond laser pulses, Science **282**, 919 (1998).

[26] X. Ren, V. Makhija, and V. Kumarappan, Multipulse Three-Dimensional Alignment of Asymmetric Top Molecules, Phys. Rev. Lett. **112**, 173602 (2014).
[27] X. Xie, J. Dai, and X.-C. Zhang, Coherent Control of THz Wave Generation in Ambient Air, Phys. Rev. Lett. **96**, 075005 (2006).
[28] M. Faraday, *Faraday's Diary of Experimental Investigation* (Royal Institution of Great Britain, London, 2008).
[29] V. Gasparian, M. Ortuno, J. Ruiz, and E. Cuevas, Faraday Rotation and Complex-Valued Traversal Time for Classical Light Waves, Phys. Rev. Lett. **75**, 2312 (1995).
[30] See Supplemental Material at http://link.aps.org/supplemental/10.1103/PhysRevApplied.6.024012 for the relation between Faraday rotation and group velocity (Sec. I), the parameters of the calculations (Sec. II), and the cross-correlation experimental setup (Sec. III).
[31] M. Inoue, K. Arai, T. Fujii, and M. Abe, One-dimensional magnetophotonic crystals, J. Appl. Phys. **85**, 5768 (1999).
[32] A. A. Fedyanin, T. Yoshida, K. Nishimura, G. Marowsky, M. Inoue, and O. A. Aktsipetrov, Nonlinear magneto-optical Kerr effect in gyrotropic photonic band gap structures: Magneto-photonic microcavities, J. Magn. Magn. Mater. **258**, 96 (2003).
[33] M. Levy and R. Li, Polarization rotation enhancement and scattering mechanisms in waveguide magnetophotonic crystals, Appl. Phys. Lett. **89**, 121113 (2006).
[34] A. B. Khanikaev, A. B. Baryshev, P. B. Lim, H. Uchida, M. Inoue, A. G. Zhdanov, A. A. Fedyanin, A. I. Maydykovskiy, and O. A. Aktsipetrov, Nonlinear Verdet law in magneto-photonic crystals: Interrelation between Faraday and Borrmann effects, Phys. Rev. B **78**, 193102 (2008).
[35] M. Soljačić and J. D. Joannopoulos, Enhancement of nonlinear effects using photonic crystals, Nat. Mater. **3**, 211 (2004).
[36] M. G. Martemyanov, E. M. Kim, T. V. Dolgova, A. A. Fedyanin, O. A. Aktsipetrov, and G. Marowsky, Third-harmonic generation in silicon photonic crystals and microcavities, Phys. Rev. B **70**, 073311 (2004).
[37] C. Monat, D. Corcoran, M. Ebnali-Heidari, C. Grillet, B. J. Eggleton, T. P. White, L. O'Faolain, and T. F. Krauss, Slow light enhancement of nonlinear effects in silicon engineered photonic crystal waveguides, Opt. Express **17**, 2944 (2009).
[38] J. Li, L. O'Faolain, I. H. Rey, and T. F. Krauss, Four-wave mixing in photonic crystal waveguides: Slow light enhancement and limitations, Opt. Express **19**, 4458 (2011).
[39] R. Iliew, C. Etrich, T. Pertsch, F. Lederer, and Y. S. Kivshar, Huge enhancement of backward second-harmonic generation with slow light in photonic crystals, Phys. Rev. A **81**, 023820 (2010).
[40] N. A. Mortensen and S. Xiao, Slow-light enhancement of Beer-Lambert-Bouguer absorption, Appl. Phys. Lett. **90**, 141108 (2007).
[41] M. L. Povinelli, M. Ibanescu, S. G. Johnson, and J. D. Joannopoulos, Slow-light enhancement of radiation pressure in an omnidirectional-reflector waveguide, Appl. Phys. Lett. **85**, 1466 (2004).
[42] J. F. McMillan, X. Yang, N. C. Panoiu, R. M. Osgood, and C. W. Wong, Enhanced stimulated Raman scattering in slow-light photonic crystal waveguides, Opt. Lett. **31**, 1235 (2006).
[43] M. S. Shahriar, G. S. Pati, R. Tripathi, V. Gopal, M. Messall, and K. Salit, Ultrahigh enhancement in absolute and relative rotation sensing using fast and slow light, Phys. Rev. A **75**, 053807 (2007).
[44] H. Ramezani, S. Kalish, I. Vitebskiy, and T. Kottos, Unidirectional Lasing Emerging from Frozen Light in Nonreciprocal Cavities, Phys. Rev. Lett. **112**, 043904 (2014).
[45] H. Kato, T. Matsushita, A. Takayama, M. Egawa, K. Nishimura, and M. Inoue, Theoretical analysis of optical and magneto-optical properties of one-dimensional magnetophotonic crystals, J. Appl. Phys. **93**, 3906 (2003).
[46] A. V. Chetvertukhin, M. I. Sharipova, A. G. Zhdanov, T. B. Shapaeva, T. V. Dolgova, and A. A. Fedyanin, Femtosecond time-resolved Faraday rotation in thin magnetic films and magnetophotonic crystals, J. Appl. Phys. **111**, 07A944 (2012).
[47] A. V. Kimel, A. Kirilyuk, P. A. Usachev, R. V. Pisarev, A. M. Balbashov, and Th. Rasing, Ultrafast non-thermal control of magnetization by instantaneous photomagnetic pulses, Nature (London) **435**, 655 (2005).
[48] J.-Y. Bigot, M. Vomir, and E. Beaurepaire, Coherent ultrafast magnetism induced by femtosecond laser pulses, Nat. Phys. **5**, 515 (2009).
[49] A. I. Musorin, P. V. Perepelkin, M. I. Sharipova, A. V. Chetvertukhin, T. V. Dolgova, and A. A. Fedyanin, Polarization sensitive correlation spectroscopy of faraday effect femtosecond dynamics, Bull. Russ. Acad. Sci. Phys. **78**, 43 (2014).
[50] K. W. Hipps and G. A. Crosby, Applications of the photoelastic modulator to polarization spectroscopy, J. Phys. Chem. **83**, 555 (1979).
[51] P. Hansen and J.-P. Krumme, Magnetic and magneto-optical properties of garnet films, Thin Solid Films **114**, 69 (1984).
[52] P. Hansen, C.-P. Klages, J. Schuldt, and K. Witter, Magnetic and magneto-optical properties of bismuth-substituted lutetium iron garnet films, Phys. Rev. B **31**, 5858 (1985).
[53] L. Gao, F. Lemarchand, and M. Lequime, Refractive index determination of SiO_2 layer in the UV/VIS/NIR range: Spectrophotometric reverse engineering on single and bi-layer designs, J. Eur. Opt. Soc. **8**, 13010 (2013).
[54] L. Gao, F. Lemarchand, and M. Lequime, Exploitation of multiple incidences spectrometric measurements for thin film reverse engineering, Opt. Express **20**, 15734 (2012).
[55] A. K. Zvezdin and V. A. Kotov, *Modern Magneto-Optics and Modern Magneto-Optic Materials* (Institute of Physics Publishing, Bristol, United Kingdom, 1997).
[56] M. R. Shcherbakov, P. P. Vabishchevich, A. Yu. Frolov, T. V. Dolgova, and A. A. Fedyanin, Femtosecond intrapulse evolution of the magneto-optic Kerr effect in magnetoplasmonic crystals, Phys. Rev. B **90**, 201405 (2014).
[57] M. J. Steel, M. Levy, and R. M. Osgood, Photonic bandgaps with defects and the enhancement of Faraday rotation, J. Lightwave Technol. **18**, 1297 (2000).
[58] K. Nakamura, H. Takagi, T. Goto, P. B. Lim, H. Horimai, H. Yoshikawa, V. M. Bove, and M. Inoue, Improvement of

diffraction efficiency of three-dimensional magneto-optic spatial light modulator with magnetophotonic crystal, Appl. Phys. Lett. **108**, 022404 (2016).

[59] R. Isogai, Y. Nakamura, H. Takagi, T. Goto, P. B. Lim, and M. Inoue, Thermomagnetic writing into magnetophotonic microcavities controlling thermal diffusion for volumetric magnetic holography, Opt. Express **24**, 522 (2016).

[60] N. K. Dissanayake, M. Levy, A. A. Jalali, and V. J. Fratello, Gyrotropic band gap optical sensors, Appl. Phys. Lett. **96**, 181105 (2010).